

Laser Trapping-Picosecond Fluorescence Microspectroscopy of Single Microdroplets under High Pressure: Droplet-Size and Pressure Effects

Fumihiko Kitagawa and Noboru Kitamura*

Division of Chemistry, Graduate School of Science, Hokkaido University, Sapporo 060-0810

(Received August 27, 2001)

A laser trapping picosecond fluorescence microspectroscopy system was combined with a high pressure cell to study droplet size and pressure effects on chemical phenomena in single micrometer-sized oil droplets. When a rectangular capillary tube was used as a pressure cell, single oil droplets were easily and stably trapped by a 1064-nm laser beam even under high pressure. The developed system enabled us to pressurize a sample emulsion as high as 75 MPa; such pressure was enough to induce pressure and droplet-size effects on the fluorescence dynamics of an Acridine Orange derivative (C_{12}-AO^+) in single oil droplets. In particular, droplet-size effects on the fluorescence dynamics were pronounced with an increase in static pressure. Possible origins of the pressure and droplet-size effects were discussed.

Chemical processes *in* or *across* a micrometer-sized droplet/solution interface should be different from those at a flat liquid/liquid interface. In particular, the surface area ($A = 4\pi r^2$)/volume ($V = (4/3)\pi r^3$) ratio ($A/V \sim 1/r$) of a droplet increases with a decrease in the droplet size (r = droplet radius). The roles of the interface become more important with increasing A/V ratio of a droplet, so that various phenomena are expected to show droplet-size effects. In a series of our publications, we reported that several chemical reactions and processes *in* a micrometer-sized droplet or *across* a droplet/solution interface were dependent on the droplet size, as demonstrated by electrochemical and steady-state/picosecond fluorescence spectroscopy techniques[1] combined with laser trapping of single microdroplets. As an example, we reported that the rate of electron transfer[2,3] or mass transfer[4] across a single-oil-droplet/water interface showed a characteristic droplet-size dependence at the droplet diameter (d) below 10 μm. The fluorescence lifetime of Rhodamine 6G in single ethylene glycol/water microdroplets dispersed in a polymer matrix also exhibits droplet size effects; the lifetime becomes shorter with decreasing d at $d < 10$ μm.[5] These results have been explained primarily by the increase in the A/V ratio of the droplet with a decrease in d. Nonetheless, the molecular-level mechanisms of the droplet-size effects, in particular, the roles of the droplet/solution interfacial structures in the size effects have not been revealed.

Despite the wealth of interest in microdroplet chemistry, the relevant experimental methods are still limited since a manipulation method for individual droplets in solution must be combined with an analytical technique: absorption and fluorescence spectroscopy, fluorescence dynamics and electrochemical techniques. In order to obtain further information about the droplet-size effects, a new experimental approach should be introduced. Among various parameters influencing droplet/solution interfacial structures, we focused on pressure effects on chemical phenomena in single droplets. If an appropriate external static pressure is applied, microdroplet/solution interfacial structures would be perturbed without an appreciable change in the solution properties of the droplet itself. Therefore, to understand further characteristic behaviors of the chemistry in microdroplets, we think external pressure could be one of the important parameters to be considered. In this study, we developed for the first time a laser trapping fluorescence dynamic microspectroscopy system combined with a high pressure system. On the basis of the developed system, we demonstrate pressure-induced microdroplet-size effects on the fluorescence lifetime of an acridine orange derivative in single microdroplets. The results are discussed in terms of the microdroplet/water interfacial structures.

Experimental

Materials and Sample Preparations. Acridine orange-10-dodecyl bromide (C_{12}-AO^+Br^-, Molecular Probes Inc.) and deuterium oxide (D_2O, Wako Pure Chemical Industries Ltd., 99.9%) were used without further purification. Perylene (Pe, Aldrich Chemical Co., Inc., 99+%) and ferrocene (Fc, Tokyo Kasei Kogyo Co., Ltd., S grade) were purified by recrystallization from toluene and methanol, respectively, followed by vacuum sublimation. Tributyl phosphate (TBP, Tokyo Kasei Kogyo Co., Ltd., GR grade) was purified by vacuum distillation after washing successively with an aqueous sodium hydroxide solution and water. As oil-in-water sample emulsions, D_2O-saturated TBP containing an appropriate dye(s) was dispersed in an oil-saturated D_2O with a volume ratio (oil/water) of 0.004. Since H_2O absorbs 1064-nm laser light, we used D_2O as a medium.[6]

Apparatus. Fig. 1 shows an experimental set up for laser trapping-microspectroscopy of single microdroplets under high pressure. A rectangular fused-silica capillary tube (Polymicro Tech., Inc., Square Flexible Fused Silica Capillary Tubing, i.d. 100 μm, o.d. 375 μm) was used as a pressure cell. A non-pulsation pump (GL Science, PUS3) was connected with the fused-silica capillary tube via a stainless steel tube. Pressure in the cell was measured by a pressure gauge (Nagano Keiki Co., Ltd., AE10-193) connected at the downstream side of the capillary tube.

Details of a laser trapping/picosecond time-resolved mi-

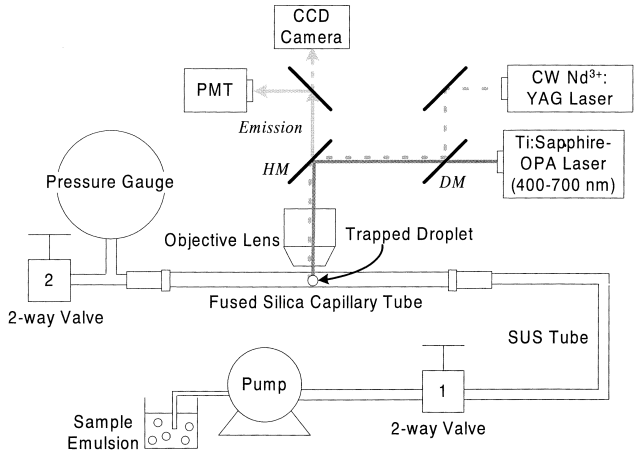

Fig. 1. Block diagram of a laser-trapping/picosecond time-resolved microspectroscopy system under high pressure: PMT; photomultiplier, HM; half-mirror, DM; dichroic mirror.

crospectroscopy system have been described elsewhere.[5] Briefly, excitation laser pulses (Coherent, 480 nm, repetition rate = 100 kHz, FWHM = 150 fs) polarized horizontally were introduced to a confocal optical microscope (OLYMPUS, BX-50) coaxially with a 1064-nm laser beam for trapping (CW Nd^{3+}: YAG laser, Spectron, SL902T), and irradiated to a laser-trapped droplet (spot size for excitation ~3 μm) through an oil-immersion objective lens (×100, N.A. = 1.35). The fluorescence from the trapped droplet was collected by the same objective lens, led to a microchannel-plate photomultiplier (Hamamatsu, R3809U-50) equipped with a monochromator (Jobin Ybon, H-20), and then analyzed by a single-photon counting module (Edinburgh Instruments, SPC-300). All the experiments were performed under aerated conditions in a temperature-controlled room (21 °C).

The interfacial tension of a TBP/D_2O system was measured by a pendant drop method. The shape of a pendant droplet was monitored by a CCD camera, and the digitized images were transferred to a microcomputer to calculate the interfacial tension value.[7]

Results and Discussion

Laser Trapping-Picosecond Fluorescence Spectroscopy under High Pressure. In order to trap a microdroplet stably by a 1064-nm laser beam, the use of an oil-immersion objective lens having a high numerical aperture is desired. However, since such an objective has a very short working distance (~200 μm), commercially available high-pressure cells (i.e., diamond anvil) cannot be used in the present purpose. Therefore, we used a submillimeter-sized fused-silica capillary tube as a pressure cell. When laser trapping of a single-oil-droplet in water was conducted by using a cylindrical capillary tube as a cell, however, an image of a trapped droplet was distorted considerably as shown in Fig. 2(*a*), because of the tube acting as a concavo-convex lens. Furthermore, trapping of a droplet needed high laser power even at atmospheric pressure, owing to reflection and scattering of the laser beam at the surface of the cylindrical tube. By using a rectangular fused-silica capillary tube as a pressure cell, on the other hand, a clear image of a droplet was obtained (Fig. 2(*b*)), so that, optical loss of the beam in the rectangular tube was almost neglected, therefore,

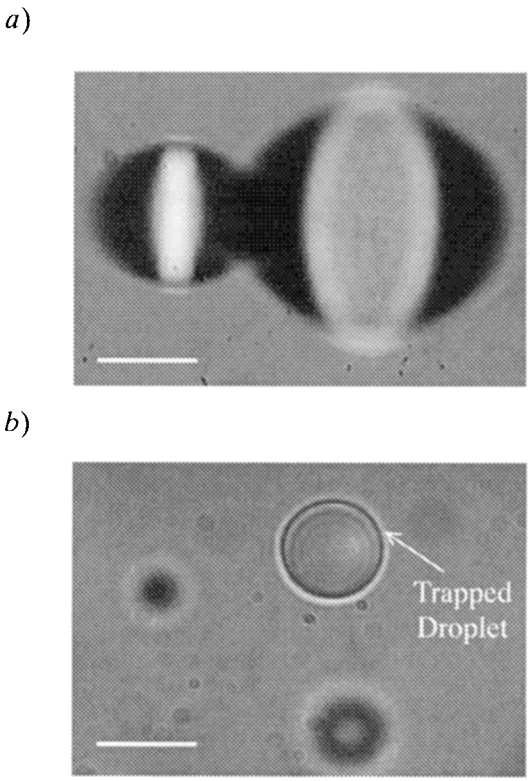

Fig. 2. Photographs of micro-oil-droplets in cylindrical (*a*) and in rectangular tubes (*b*). Scale bar is 10 μm.

we succeeded in stable and strong trapping of an oil droplet with laser power as low as 100 mW even under high pressure.

In actual experiments, the following procedures were employed to trap and analyze single microdroplets under high pressure. A sample emulsion was introduced to a fused silica capillary tube by using a pump, and the emulsion was pressurized by the same pump. Then valves 1 and 2 were closed to hold at a desired pressure. In order to equilibrate the sample emulsion at a given pressure, the emulsion was allowed to stand for over 30 min prior to spectroscopic measurements. A single microdroplet in the tube was then trapped by a 1064-nm laser beam, and the fluorescence from the trapped droplet was analyzed by a time-correlated single-photon counting technique. On the basis of such a system and procedures, we could pressurize a sample solution as high as 75 MPa. Although the applied pressure decreased by ~3% during the first 1 h, it reached a constant value: ±2%.

In order to test the performance of the developed system, we studied pressure effects on fluorescence dynamics in single TBP microdroplets. In the case of investigating the fluorescence dynamics in micrometer-sized oil droplet dispersed in water, a probe molecule is need to have insoluble nature in water and to show simple photodynamics even in moderately high concentration. In such a point of view, we choose perylene (Pe) as a probe molecule for this purpose. It is known that Pe having a high fluorescence quantum yield (0.94 in ethanol)[8] is photochemically stable and does not produce an excimer/dimer even at a high concentration, therefore, the molecule is very suitable for investigating the fluorescence dynamics in an oil-droplet/water system. Fig. 3 shows the fluorescence dy-

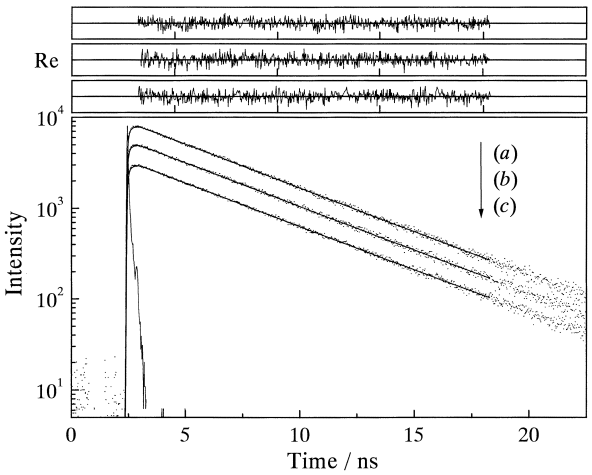

Fig. 3. Fluorescence decay profiles of Pe in a bulk (*a*) and single TBP microdroplets (d = 3 μm) at 0.1 (*b*) and 60 MPa (*c*). The solid curve shows the best fit by a single exponential function.

namics of Pe in a bulk TBP solution (1.0×10^{-6} M, (*a*)) and in individual TBP microdroplets dispersed in D_2O (5.0×10^{-4} M, 0.1 MPa (*b*) and 60 MPa (*c*)). It is worth emphasizing that the decay profiles observed for both bulk solution and droplets are always best fitted by single exponential functions. The fluorescence lifetime (τ) of Pe in each TBP droplet was almost constant at 4.55–4.60 ns irrespective of the droplet diameter (d), and agreed very well with that determined in a bulk solution (4.60 ns). Furthermore, the τ value remained practically unchanged with a variation of pressure: 0.1–60 MPa. Generally, an application of static pressure (P) to a solution renders an increase in the solution viscosity. The absence of a pressure effect on τ is thus explained by either a small viscosity change of the oil by P or by the nature of τ as insensitive to the viscosity. In order to check such possibilities, we studied fluorescence quenching of Pe by ferrocene (Fc) in single TBP droplets. Since fluorescence quenching of Pe by Fc proceeds at a diffusion-controlled rate, the relevant quenching rate constant (k_q) should decrease under an applied pressure compared to that at atmospheric pressure. Indeed, the fluorescence decay time of Pe in the presence of Fc (5.0×10^{-2} M) was ~1.95 ns at 0.1 MPa, while that increased to ~2.30 ns at 60 MPa (data are not shown here). According to the Stern–Volmer relation and the diffusion theory, the increase in τ by P corresponds to the decrease in k_q by a 1.3-fold and to the increase in the viscosity of TBP from 3.39 cP (0.1 MPa, 25 °C) to 4.40 cP (60 MPa). The results demonstrate that a static pressure can be certainly applied to the sample emulsion in the present system. Furthermore, we conclude that the fluorescence lifetime of Pe in the absence of a quencher is insensitive to a viscosity change for a pressure increase up to 60 MPa.

Droplet-Size Effects on the Fluorescence Dynamics of Acridine Orange in Single TBP Droplets. Acridine orange-10-dodecyl bromide (C_{12}-AO^+) is surface active and adsorbs on a droplet/water interface, so that we expected that the fluorescence characteristic of the dye would provide information about the interfacial properties of a micrometer-sized droplet. Thus, we conducted fluorescence dynamic spectroscopy of C_{12}-AO^+ in single TBP droplets dispersed in D_2O. Fig. 4 shows a typical example of the fluorescence decay profiles of C_{12}-AO^+ (2.0×10^{-3} M) in individual TBP microdroplets with ((*a*), 60 MPa) and without an applied pressure ((*b*)). Although the decay profile observed in a bulk solution (2.0×10^{-3} M) could be fitted by a single exponential function (τ = 1.15 ns), those observed in single droplets were best-fitted by double exponential functions (monitoring wavelength; 580 nm). The short lifetime component (τ_S = ~1.2 ns) coincided with that in the bulk solution, while a long lifetime component (τ_L = ~9 ns) was observed in the TBP droplets. The double exponential decay of the fluorescence is reasonably explained by dimer formation of C_{12}-AO^+ in the TBP droplets. It has been reported that an aqueous concentrated acridine orange solution shows dimer emission at around 620 nm and its lifetime is as long as 13 ns.[9] In the present case, no τ_L component was observed when the fluorescence from the droplet was monitored at 525 nm. Since the C_{12}-AO^+ fluorescence decays single exponentially in a bulk TBP solution, the τ_L component observed in the microdroplets at 580 nm could be responsible for the dimer adsorbed on the droplet/water interface owing to the surface active nature of C_{12}-AO^+.

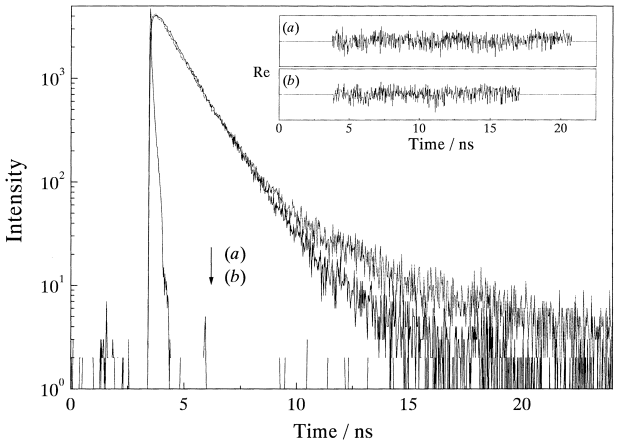

Fig. 4. Fluorescence decay profiles of C_{12}-AO^+ in single TBP microdroplets (d = 3 μm) at 60 (*a*) and 0.1 MPa (*b*).

The dimer formation of C_{12}-AO^+ at the TBP droplet/water interface indicates that its efficiency should increase with a decrease in d, as demonstrated previously for dimer formation of Malachite Green in single water droplets dispersed in an oil phase.[10,11] It has been reported that adsorption of Malachite Green at the water droplet/oil interface facilitates the dimer formation owing to the increase in the surface concentration of the dye; this produces a decrease in the monomer concentration in the droplet interior. As a result, the efficiency of dimer formation is dependent on the A/V ratio of the droplet. In order to test whether a context such as mentioned above holds or not in the present case, we conducted laser trapping–fluorescence spectroscopy on various-sized TBP droplets at several applied pressures. The decay profiles monitoring at 580 nm were analyzed successfully by the sum of τ_S (~1.2 ns) and τ_L (~9 ns)

$$I(t) = A_s\exp\left(\frac{-t}{\tau_S}\right) + A_L\exp\left(\frac{-t}{\tau_L}\right) \quad (1)$$

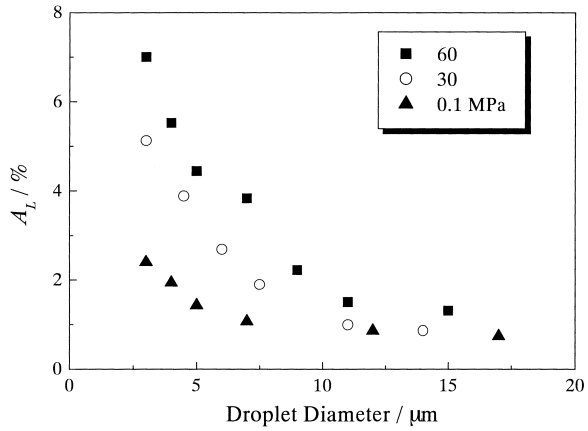

Fig. 5. Droplet-size and pressure effects on A_L in single TBP droplets at 60 (closed squares), 30 (open circles), and 0.1 MPa (closed triangles).

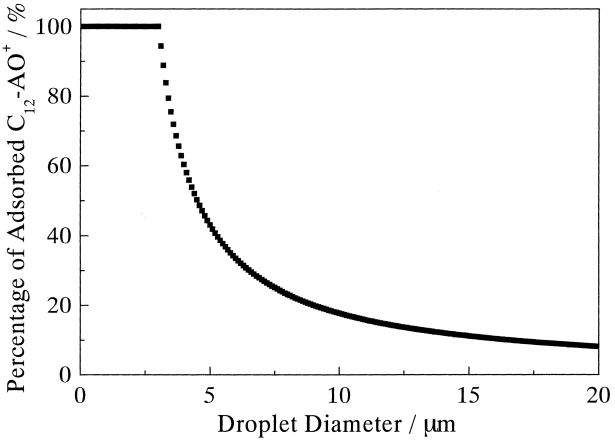

Fig. 7. Droplet size dependence of the relative percentage of the adsorbed C_{12}-AO^+ molecules on the interface to the monomer concentration in the droplet interior.

irrespective of d and P, with the amplitudes of the decay components (A_L and A_S, respectively) being varied. Thus, the results were summarized as droplet-size and pressure dependencies of the amplitude of the τ_L component (A_L), as shown in Fig. 5. As seen in the figure, A_L and, therefore, the contribution of the C_{12}-AO^+ dimer to the overall dye molecules increased with decreasing the droplet diameter at a given P. The results prove adsorption and subsequent dimer formation of C_{12}-AO^+ at the droplet/water interface, and the dimer formation is facilitated by the decrease in d through the increase in the A/V ratio of the droplet: *micrometer droplet-size effects*. To estimate the amount of adsorbed C_{12}-AO^+, interfacial tension measurements were conducted; the results are summarized in Fig. 6. The C_{12}-AO^+ concentration dependence of the interfacial tension was analyzed by the Gibbs equation and the Langmuir isotherm. We estimated the saturated amount of adsorbed C_{12}-AO^+ on the TBP/D_2O interface to be $\Gamma_\infty = 5.0\times10^{-11}$ mol/cm^2.[12] Furthermore, we calculated the droplet size dependence of the relative percentage of the adsorbed C_{12}-AO^+ molecules on the interface to the mole number of the monomer in the droplet interior by using the relevant A/V and Γ_∞ values, as shown in Fig. 7. The relative percentage of the adsorbed molecules increased with decreasing d. For the droplets with $d <$ 10 μm, it is worth noting that the percentage increases very sharply from 18 to 100% on going from $d = 10$ to 3 μm. Therefore, the d effects on A_L or the dimer formation in Fig. 5 are explained by the increase in the relative percentage of the adsorbed molecules on the interface to the monomer in the droplet interior through that in the A/V ratio of the droplet.

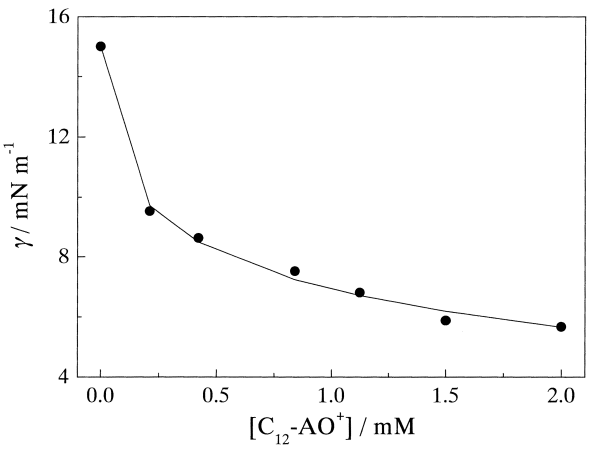

Fig. 6. C_{12}-AO^+ concentration dependence of the interfacial tension in a TBP/D_2O system. The solid curve represents the best fit to the Gibbs equation and Langmuir isotherm.

Pressure-Induced Droplet-Size Effects on Dimer Formation of C_{12}-AO^+ in Single TBP Droplets. The most important result of the study is large facilitation of the droplet-size effects by P, in particular for the droplets with $d <$ 10 μm (Fig. 5). For the droplet with $d = 3$ μm, as an example, A_L at 60 MPa was three times larger than that at 0.1 MPa; dimer formation at the droplet/water interface is enhanced by an external pressure. Under the present experimental conditions, the physical properties of TBP itself do not change appreciably with the pressure (~60 MPa). Actually, the volume change of the emulsion sample by pressurization to 60 MPa is only ~3%,[13] so that the increase in the dimer formation efficiency by P cannot be explained by that in the dye concentration in the droplet. An applied pressure would influence more or less the monomer–dimer equilibrium of C_{12}-AO^+ in the TBP droplet, and small but finite volume contraction ($\Delta V \sim -10$ cm^3/mol in an aqueous solution)[14] will favor the dimer formation. Nonetheless, the ~3-fold increase in A_L at 60 MPa ($d = 3$ μm) compared to the value at 0.1 MPa would not be explained by a P effect on the equilibrium. Furthermore, although the solvent properties such as viscosity, refractive index, and so forth are also dependent on P, these parameters would not govern directly the dimer formation efficiency. Pressure effects on adsorption behavior of a surface active molecule at an oil/water interface have been reported.[15] According to the literature, an interfacial tension is not varied up to 100 MPa. Therefore, it is concluded that the adsorption equilibrium of C_{12}-AO^+ does not change appreciably under the present condition (0.1–60 MPa). The P effects on the dimer formation efficiency do not originate from an adsorption equilibrium change with P.

We consider that variations of the interfacial structures (including the adsorption behavior of a probe) of the TBP droplet

are a possible origin of the pressure effects on A_L in Fig. 5. We reported the structures of flat water/oil interfaces on the basis of total-internal-reflection fluorescence spectroscopy, and demonstrated that the interfacial structures (thickness/roughness) were influenced by the solubility of water in an oil.[16] Namely, when the solubility of water in an oil is high, the relevant oil/water interface becomes rougher and thicker than the system with a low water solubility. The solubility of water in an oil increases with increasing P, so that a TBP droplet/water interface is considered to become thicker under an applied pressure compared to that at an atmospheric pressure. A thick droplet/water interfacial layer would be favorable for dimer formation, since the increase in the water content in the interfacial layer brings about a hydrophobic interaction between C_{12}-AO^+. We consider that this is the primary origin of the P effects on A_L in Fig. 5. These discussions remind us our previous work on an electron transfer (ET) reaction across a single TBP droplets/water interface; we found a droplet-size dependence of the ET rate constant at d $<$ 5 μm, while an addition of a small amount of sodium dodecyl sulfate (SDS) to the system induced disappearance of the droplet-size effect.[3] As reported previously in detail, the results were explained by adsorption of SDS on the TBP droplet surface and the resultant decrease in the thickness of the surface layer of the droplet through pushing out the water molecules in the layer to the water phase. We consider that the droplet/water interfacial structures, particularly the interfacial thickness, is a very important factor governing the chemical and physical dynamics of a solute in microdroplets.

Conclusions

By using a laser trapping picosecond fluorescence microspectroscopy system combined with a high pressure cell, we investigated pressure and droplet-size effects on the fluorescence dynamics of C_{12}-AO^+ in single micrometer-sized TBP droplet dispersed in D_2O. The contribution of the C_{12}-AO^+ dimer to the overall dye molecules increased with decreasing the droplet diameter through the increase in the A/V ratio of the droplet. The most important result of the study is large facilitation of the droplet-size effects by pressure, in particular for the droplets with $d < 10$ μm. The results will be explained by a relatively thick interfacial layer at high pressure compared to that at atmospheric pressure. A study on a pressure dependence of photodynamics of a dye is a very powerful tool to elucidate the chemistry of the micrometer-sized droplets.

N. K. acknowledges a Grant-in-Aid from the Ministry of Education, Science, Sports and Culture, for the Priority Research Area B on "Laser Chemistry of Single Nanometer Organic Particles" (No. 10207201) for partial support of this research. The authors also acknowledge Prof. H.-B. Kim at the University of Tokyo for fruitful discussions.

References

1 H. Masuhara, F. C. De Schryver, N. Kitamura, and N. Tamai, "Microchemistry, Spectroscopy and Chemistry in Small Domains," North-Holland, Amsterdam (1994).

2 K. Nakatani, K. Chikama, H.-B. Kim, and N. Kitamura, *Chem. Phys. Lett.*, **237**, 133 (1995).

3 K. Chikama, K. Nakatani, and N. Kitamura, *Bull. Chem. Soc. Jpn.*, **71**, 1065 (1998).

4 K. Nakatani, M. Sudo, and N. Kitamura, *J. Phys. Chem. B*, **102**, 2908 (1998).

5 S. Habuchi, H.-B. Kim, and N. Kitamura, *J. Photochem. Photobiol. A*, **133**, 189 (2000).

6 H. Ishikawa, H. Misawa, N. Kitamura, R. Fujisawa, and H. Masuhara, *Bull. Chem. Soc. Jpn.*, **69**, 59 (1996).

7 W. Adamson, "Physical Chemistry of Surfaces," John Wiley & Sons, New York (1990).

8 W. R. Dawson and M. W. Windsor, *J. Phys. Chem.*, **1996**, 3251 (1968).

9 J. Knof, F. J. Theiss, and J. Waber, *Z. Naturforsch.*, **33a**, 98 (1978).

10 H. Yao, H. Ikeda, and N. Kitamura, *Langmuir*, **13**, 997 (1996).

11 H. Yao, Y. Inoue, H. Ikeda, K. Nakatani, H.-B. Kim, and N. Kitamura, *J. Phys. Chem.*, **100**, 1494 (1996).

12 H. Watarai, Y. Horii, and M. Fujishima, *Bull. Chem. Soc. Jpn.*, **61**, 1159 (1988).

13 P. W. Bridgman, *Proc. Am. Acad. Arts Sci.*, **1**, 67 (1932).

14 K. Suzuki and M. Tsuchiya, *Bull. Chem. Soc. Jpn.*, **44**, 967 (1971).

15 T. Takiue, T. Toyomasu, N. Ikeda, and M. Aramoto, *J. Phys. Chem. B*, **103**, 6547 (1999).

16 S. Ishizaka, S. Habuchi, H.-B. Kim, and N. Kitamura, *Anal. Chem.*, **71**, 3382 (1999).